1521-0103/12/3423-696–708$25.00
THE JOURNAL OF PHARMACOLOGY AND EXPERIMENTAL THERAPEUTICS Vol. 342, No. 3

195479/3786798
JPET 342:696–708, 2012

Intestinal Transport of Aminopterin Enantiomers in Dogs and Humans with Psoriasis Is Stereoselective: Evidence for a Mechanism Involving the Proton-Coupled Folate Transporter

Alan Menter, Breck Thrash, Christina Cherian, Larry H. Matherly, Lei Wang, Aleem Gangjee, Joel R. Morgan, Dean Y. Maeda, Aaron D. Schuler, Stuart J. Kahn, and John A. Zebala

Baylor Research Institute, Dallas, Texas (A.M., B.T.); Barbara Ann Karmanos Cancer Institute, Wayne State University School of Medicine, Detroit, Michigan (C.C., L.H.M.); Division of Medicinal Chemistry, Graduate School of Pharmaceutical Sciences, Duquesne University, Pittsburgh, Pennsylvania (L.W., A.G.); and Syntrix Biosystems Inc., Auburn, Washington (J.R.M., D.Y.M., A.D.S., S.J.K., J.A.Z.)

Received April 12, 2012; accepted May 30, 2012

ABSTRACT

N-[4-[[(2,4-diamino-6-pterdinyl)methyl]amino]benzoyl]-L/D-glutamic acid (L/D-AMT) is an investigational drug in phase 1 clinical development that consists of the L-and D-enantiomers of aminopterin (AMT). L/D-AMT is obtained from a novel process for making the L-enantiomer (L-AMT), a potent oral anti-inflammatory agent. The purpose of these studies was to characterize oral uptake and safety in the dog and human of each enantiomer alone and in combination and provide in vitro evidence for a mechanism of intestinal absorption. This is the first report of L /D-AMT in humans. In dogs ($n = 40$) orally dosed with L-AMT or D-AMT absorption was stereoselective for the L-enantiomer (6- to 12-fold larger peak plasma concentration after oral administration and area under the plasma concentration-time curve at 0–4 h; $p < 0.001$). D-AMT was not toxic at the maximal dose tested (82.5 mg/kg), which was 100-fold larger than the maximal nonlethal L-AMT dose (0.8 mg/kg). Dogs ($n = 10$) and humans with psoriasis ($n = 21$) orally administered L-AMT and L /D-AMT at the same L-enantiomer dose resulted in stereoselective absorption (absent D-enantiomer in plasma), bioequivalent L-enantiomer pharmacokinetics, and equivalent safety. Thus, the D-enantiomer in L/D-AMT did not perturb L-enantiomer absorption or alter the safety of L-AMT. In vitro uptake by the human proton-coupled folate transporter (PCFT) demonstrated minimal transport of D-AMT compared with L-AMT, mirroring the in vivo findings. Enantiomer selectivity by PCFT was attributable almost entirely to decreased binding affinity rather than changes in transport rate. Collectively, our results demonstrate a strong in vitro-in vivo correlation implicating stereoselective transport by PCFT as the mechanism underlying stereoselective absorption observed in vivo.

Introduction

Aminopterin (AMT) is an oral antifolate that was marketed by Lederle Laboratories in the United States between 1953 and 1964 for pediatric acute leukemia (Folsom et al., 1965). During this period, AMT was used off-label to treat thousands of psoriatic subjects, being favored by dermatologists over the other antifolate then marketed concurrently by Lederle, methotrexate (MTX) (Rees et al., 1964). Lederle ceased marketing AMT in 1964 for reasons not completely known, but evidence points to difficulties in its manufacture (Rees et al., 1964). As a result, clinicians turned to MTX. In 1971, the Food and Drug Administration formally approved MTX for the treatment of severe psoriasis. Over the ensuing decades MTX became the backbone of therapy for inflammatory diseases, including psoriasis, psoriatic arthritis, and rheumatoid arthritis, diseases that affect more than 100

This work was supported in part by Syntrix Biosystems; the National Institutes of Health National Institute of Arthritis, Musculoskeletal, and Skin [Grant 1R43AR056547]; the National Institutes of Health National Institute of Allergy and Infectious Diseases [Grant 1R43AI68282]; and the National Institutes of Health National Cancer Institute [Grants 1R01CA53535, 1R01CA152316].
Article, publication date, and citation information can be found at http://jpet.aspetjournals.org.
http://dx.doi.org/10.1124/jpet.112.195479.

ABBREVIATIONS: AMT, aminopterin; AE, adverse event; AUC, area under the plasma concentration-time curve; CHO, Chinese hamster ovary; CI, confidence interval; CL, clearance; C_{max}, peak plasma concentration after oral administration; compound 1, 2-({5-[4-(2-amino-4-oxo-4,7-dihydro-3*H*-pyrrolo[2,3-*d*]pyrimidin-6-yl)-butyl]-thiophen-2-carbonyl}-amino)-pentanedioic acid; CV, coefficient of variation; DMSO, dimethyl sulfoxide; DPBS, Dulbecco's phosphate-buffered saline; GFR, glomerular filtration rate; K_t, whole-cell Michaelis constant; LC-MS/MS, liquid chromatography/tandem mass spectrometry; L/D-AMT, *N*-[4-[[(2,4-diamino-6-pterdinyl)methyl]amino]benzoyl]-L/D-glutamic acid; LD-AMT-d_3, deuterated LD-AMT-α,γ,γ-d_3; MES, 4-morpholineethanesulfonic acid; MTX, methotrexate; NA, no addition; PCFT, proton-coupled folate transporter; PMX, pemetrexed; PT523, N^{α}-(4-amino-4-deoxypteroyl)-N^{δ}-hemipthalolyl-L-ornithine; QC, quality control; SAE, serious adverse event; T_{max}, time to C_{max}; V_D, apparent volume of distribution.

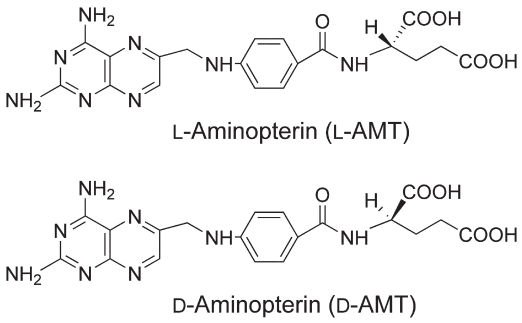

Fig. 1. Chemical structure of L-AMT (top; *N*-[4-[[(2,4-diamino-6-pterdinyl)methyl]amino]benzoyl]-L-glutamic acid) and D-AMT (bottom; *N*-[4-[[(2,4-diamino-6-pterdinyl)methyl]amino]benzoyl]-D-glutamic acid), each with a molecular weight of 440.4 g/mol.

million patients (Fiehn, 2009; Menter et al., 2009). Preclinical and clinical studies indicate that AMT compared with MTX has better oral bioavailability, greater cellular uptake, and less central nervous system and liver toxicity, properties that may translate into improved efficacy and/or safety (Smith et al., 1996; Ratliff et al., 1998; Cole et al., 2005, 2006, 2009). These features of AMT have resulted in renewed interest in its clinical development for oncology and inflammatory diseases (Ratliff et al., 1998; Cole et al., 2005, 2008; Olivry et al., 2007).

Chemically, AMT, or L-AMT herein, is the pure L-enantiomer *N* [4-[[(2,4-diamino-6-pterdinyl)methyl]amino]benzoyl]-L-glutamic acid (Fig. 1). We developed a novel manufacturing process more facile and efficient than the process used by Lederle that converts folic acid directly to L /D-AMT, a mixture of L-AMT and its opposite enantiomer, the new chemical entity D-AMT (Zebala, 2007). Based on favorable manufacturing and preclinical safety, L/D-AMT entered phase 1 clinical development.

Transport of the L-enantiomer in L/D-AMT across the intestine is critical to its oral delivery to the systemic circulation. The purpose of the current studies was to examine the pharmacokinetics of orally administered L-AMT, D-AMT, and L/D-AMT in canines and L-AMT and L/D-AMT in humans with moderate to severe psoriasis and determine the absorption and pharmacokinetics of the L-and D-enantiomers and whether the D-enantiomer in L/D-AMT influenced L-enantiomer pharmacokinetics. The human study herein was a clinical trial that formally tested for the statistical bioequivalence of L-AMT and L/D-AMT in patients with psoriasis. The clinical trial was a first in-human administration of the D-enantiomer, thus the assessment of safety in canine and human species was also a purpose of these studies.

Further studies with cells expressing the human proton-coupled folate transporter (PCFT; also known as SLC46A1), the major intestinal folate transporter, investigated the transport of L-AMT and D-AMT in vitro. PCFT is a proton-folate symporter at the apical brush-border membrane of the proximal small intestine that functions optimally at acidic pH by coupling the downhill flow of protons to the uphill transport of folates (Qiu et al., 2006; Nakai et al., 2007; Zhao and Goldman, 2007). The exclusive role of PCFT in intestinal folate absorption was established by demonstrating loss-of-function mutations in the PCFT of patients with the rare autosomal inherited disorder hereditary folate malabsorption (Qiu et al., 2006). At acidic pH typical of the upper intestine, the PCFT is also an efficient transporter of some [e.g., MTX and pemetrexed (PMX)], but not all [e.g., N^{α}-(4-amino-4-deoxypteroyl)-N^{δ}-hemiphthaloyl-L-ornithine (PT523)] antifolates having close structural homology to natural dietary folates.

The studies reported herein provide new information regarding the safety, systemic pharmacokinetics, and stereoselectivity of intestinal absorption of L-and D-AMT enantiomers in dogs and humans after oral dosing and demonstrate a strong in vitro-in vivo correlation implicating stereoselective transport by the PCFT as the underlying mechanism that explains the stereoselective transport of aminopterin enantiomers.

Materials and Methods

Drug Products

Each AMT enantiomer was formulated as the disodium salt. All doses are expressed as the free acid equivalent. L-AMT was synthesized as described previously (Piper and Montgomery, 1974, 1977) and provided as a powder for dissolution in water or as a tablet containing 0.70 or 0.77 mg of L-AMT. D-AMT was prepared by using the same synthesis as described for L-AMT, but using D-glutamic acid (Sigma, St. Louis, MO) in place of L-glutamic acid, and the resulting powder provided for encapsulation or dissolution in water. L/D-AMT was synthesized by the direct conversion of folic acid in a process that yields a mixture of L-and D-enantiomers in a 70:30 ratio (Zebala, 2007). The L/D-AMT thus produced was provided as a tablet containing 0.175 mg of L-isomer and 0.075 mg of D-isomer. Drug product encapsulation was in porcine gelatin capsules (Torpac, Inc., Fairfield, NJ).

Chemicals and Reagents

Unlabeled L-AMT was from Sigma. Unlabeled D-AMT was synthesized as described previously (see *Drug Products*). Unlabeled PMX was from Eli Lilly & Co. (Indianapolis, IN). Unlabeled MTX was from the Drug Development Branch, National Cancer Institute (Bethesda, MD).-({5-[4-(2-Amino-4-oxo-4,7-dihydro-3*H*-pyrrolo[2,3-*d*]pyrimidin-6-yl)-butyl]-thiophen-2-carbonyl}-amino)-pentanedioic acid (compound 1) was synthesized as described previously (Wang et al., 2010). Deuterated LD-AMT-α,γ,γ-d_3 (LD-AMT-d_3) was synthesized as described for L-AMT (see *Drug Products*), but using deuterated LD-glutamic acid-2,4,4-d_3 (Cambridge Isotope Laboratories, Inc., Andover, MA) in place of L-glutamic acid. [3′,5′,7-^{3}H]L-MTX (20 Ci/mmol), [3′,5′,7,9-^{3}H]L-AMT (38.4 Ci/mmol), [^{3}H]D-AMT (3.7 Ci/mmol), and [^{3}H]PMX (8.1 Ci/mmol) were from Moravek Biochemicals (Brea, CA). Other chemicals were the highest purities from commercial sources.

Pharmacokinetics of L-AMT, D-AMT, and L/D-AMT in Dogs

Animal use in these studies was approved by the Institutional Animal Care and Use Committees at the Illinois Institute of Technology Research Foundation (Chicago, IL) and Charles River Laboratories Preclinical Services (Redfield, AR), the sites where the animal studies were performed.

L-AMT and D-AMT Pharmacokinetics and Toxicity in Escalating Doses. Twenty-two male and 22 female beagle dogs, 5 to 6 months old, were obtained from Ridglan Farms (Mount Horeb, WI). All animals were immunized against distemper, hepatitis, parainfluenza, leptospirosis, rabies, and parvovirus by the supplier and were prophylactically administered broad-spectrum anthelmentics for internal parasites. Dogs were housed individually in pens under controlled temperature (20–25°C) and humidity (30–70%) on a 12-h light/dark cycle, fed 400 g of a controlled diet (Harlan Teklad, Madison, WI) daily, and given access to water ad libitum. Dogs were acclimated for 1 month before initiation of the study and weighed 6 to 10 kg at the initiation of dosing. L-AMT and D-AMT powders each

were dissolved in a volume of water to permit dosing of 2 ml per kilogram of body weight by gavage; vehicle controls received 2 ml of water per kilogram of body weight. Each dose and vehicle control group consisted of two males and two females. Animals were dosed on days 1 and 8. Doses of the L-enantiomer ranged from a dose having optimal anti-inflammatory activity at the low end of the range (data from canine model of inflammation not presented herein) to the minimal lethal single dose at the upper end of the range (Thiersch and Philips, 1949; Rieselbach et al., 1963). Doses of the D-enantiomer were at least 10-fold larger than the L-enantiomer doses to allow for possible poor intestinal absorption of the D-enantiomer. All animals were fasted 3 to 4 h before dosing on day 1, and food was withheld for 3 to 4 h after dosing. Blood samples for pharmacokinetic analyses were obtained from the jugular vein of all animals before and at 0.5, 1, 2, and 4 h after dosing on day 1. Blood was anticoagulated with K_2EDTA and centrifuged, and the plasma was stored at −70°C until analysis by LC-MS/MS. Toxicity was assessed through detailed clinical and physical observations performed on all animals before dosing and daily after dosing that included body weight and food consumption. All dogs received a complete necropsy that included gross and histopathologic examinations on day 16, or earlier if found dead or moribund and then euthanized. Clinical chemistry, hematology, coagulation, and urinalysis determinations were obtained on all dogs during the quarantine period (pretest) and on day 15; blood samples were obtained from the jugular or cephalic vein.

L-AMT and L/D-AMT Pharmacokinetics at the Same Dose of L-Enantiomer. Five male (12.3–13.7 kg) and five female (8.9–10.9 kg) beagle dogs age 10 to 12 months at the initiation of the study were obtained from Marshall BioResources (North Rose, NY). Dogs were housed individually in pens under controlled temperature (18–29°C) and humidity (30–70%) on a 12-h light/dark cycle, fed a controlled diet (Purina, St. Louis, MO) daily, except during periods of fasting, and given access to water ad libitum, including during fasting. One L-AMT tablet (0.77 mg of L-isomer) and four L/D-AMT tablets (0.70 mg of L-isomer and 0.30 mg of D-isomer) were separately encapsulated and given by gavage according to a randomized, single-dose, two-way crossover design. Group 1 (two males, three females) was given L-AMT on day 1 and L/D-AMT on day 8, and group 2 (three males, two females) was given L/D-AMT on day 1 and L-AMT on day 8. All animals were fasted 3 to 4 h before dosing, and food was withheld for 18 h after dosing. Blood specimens were collected via the jugular vein before and at 0.5, 1.0, 1.5, 2.0, 3.0, 6.0, 9.0, and 12.0 h after dosing. Blood was anticoagulated with K_2EDTA and centrifuged, and the plasma was stored at −70°C until analysis by achiral (for all L/D-AMT and L-AMT dosings, all nine timed collections) and chiral (for all L/D-AMT dosings, all timed collections having a value in the achiral assay above the lower limit of quantification) LC-MS/MS (see *LC-MS/MS Analysis of Plasma L-AMT and D-AMT*).

Clinical Pharmacokinetic and Bioequivalence Study of L-AMT and L/D-AMT

The phase 1 clinical trial (ClinicalTrials.gov; NCT00937027) was performed at the Baylor Research Institute (Dallas, TX) in accordance with the Declaration of Helsinki, International Conference on Harmonization Guidelines for Good Clinical Practices, and Food and Drug Administration regulations. The Baylor Research Institute Institutional Review Board approved the study protocol, and all participants were given full and adequate verbal and written information regarding the objective and procedures of the trial and the possible risks involved before inclusion in the trial.

The study was a two-arm randomized, open-label, two-period crossover trial in 22 male and female subjects with moderate to severe psoriasis, designed and powered to formally test for the bioequivalence of L-AMT and L/D-AMT (Rani, 2007). Subjects who signed an informed consent form to participate in the study underwent screening within 4 weeks of the study start date (day 0). Screening began in September 2009, and the last subject completed the study in April 2010. To participate in the trial subjects had to meet the following inclusion criteria: 1) moderate to severe psoriasis treated for ≥3 months with MTX (10–20 mg/week); 2) 18 to 74 years old; 3) body weight of 35 to 125 kg; and 4) normal hematologic, liver, and kidney function, including a glomerular filtration rate (GFR) ≥ 60 ml/min computed according to the Cockcroft-Gault formula (Cockcroft and Gault, 1976). The exclusion criteria included: 1) history of liver, interstitial lung, and inflammatory bowl diseases; 2) HIV infection or tuberculosis; 3) body mass index <18.5 or >40.0; 4) use of AMT-interacting medications (including MTX) within 2 weeks of randomization (i.e., a 2-week washout, which could include MTX); 5) pregnancy or lactation; 6) substance abuse; and 7) lack of contraception.

Each subject was to receive one L-AMT tablet (0.70 mg of L-isomer) and four L/D-AMT tablets (0.70 mg of L-isomer and 0.30 mg of D-isomer), with a 1-week washout period between doses (dose selection guided by predicted optimal anti-inflammatory L-enantiomer dose). Subjects were randomized 1:1 to two treatment arms (i.e., arm 1 and arm 2) with a computer-generated list (blocks of two). On day 0, arm 1 was administered L/D-AMT and arm 2 received L-AMT. On day 7, subjects crossed over to the other arm. Clinical safety was assessed on days 0, 7, and 14. Safety labs were collected between study days −2 and 0, between study days 5 and 7, and on study day 14 and included a complete blood count with differential, blood urea nitrogen, serum creatinine, serum aspartate aminotransferase, serum alanine aminotransferase, alkaline phosphatase, total bilirubin, albumin, total protein, and urine analysis.

The subjects were admitted to the clinic in the early morning on the same day of the study and were fasted 1 h before and 2 h after oral administration of the drug product. Food consumption before arrival at the clinic was not restricted. Pharmacokinetic samples for quantitation of L-AMT and D-AMT in plasma were obtained over 12 h after each oral dose administration of the drug product. Venous blood was collected by direct venipuncture or indwelling catheter before and at 0.5, 1.0, 1.5, 2.0, 3.0, 5.0, 7.0, 10.0, and 12.0 h after the single-dose administration of the drug product. Venous blood was collected into K_2EDTA vacutainers and centrifuged at 3000 rpm for 10 min, and the plasma was transferred to sample vials. Plasma was stored at −70°C until analysis by achiral (for all L/D-AMT and L-AMT dosings, all 10 time points) and chiral (for L/D-AMT dosings, all 10 time points in subjects 1–6, then in each of subjects 7–22, the time points with the four largest values in the achiral assay) LC-MS/MS (see *LC-MS/MS Analysis of Plasma L-AMT and D-AMT*).

Cell Culture and In Vitro Transport of L-and D-AMT by Human PCFT

PCFT- and reduced folate carrier-null MTXRIIOua^{R}2–4 (R2) Chinese hamster ovary (CHO) cells were a gift from Dr. Wayne Flintoff (University of Western Ontario, London, ON, Canada) (Flintoff and Nagainis, 1983). Cells were cultured in α-minimal essential media supplemented with 10% bovine calf serum (Invitrogen, Carlsbad, CA), 100 units/ml penicillin, 100 μg/ml streptomycin, and 2 mM L-glutamine at 37°C with 5% CO_2. Cells were periodically determined to be free of *Mycoplasma* spp. by using LookOut (Sigma). Human PCFT-expressing R2-transfected cells (R2/hPCFT4) were described previously (Desmoulin et al., 2010) and cultured as described for the R2 cells, except that 1 mg/ml G418 was added.

CHO (R2 and R2/hPCFT4) sublines were routinely grown as monolayers. Three days before transport experiments, cells were transferred to Cytostir spinners (Kimble/Kontes, Vineland, NJ) and maintained in suspension at densities of 2 to 5 × 10^5 cells/ml. Cell were collected by centrifugation and washed with Dulbecco's phosphate-buffered saline (DPBS), and the cell pellets (~2 × 10^7 cells) were suspended in transport buffer (2 ml) for cellular uptake assays. pH-dependent uptake of 0.5 μM [^{3}H]L-AMT, [^{3}H]D-AMT, and [^{3}H]PMX was assayed in cell suspensions over 1, 2, and 5 min (AMT)

or 1 min (PMX) at 37°C in HEPES-buffered saline (20 mM HEPES, 140 mM NaCl, 5 mM KCl, 2 mM $MgCl_2$, and 5 mM glucose) at pH 6.5 or 6.8 or in MES-buffered saline (20 mM MES, 140 mM NaCl, 5 mM KCl, 2 mM $MgCl_2$, and 5 mM glucose) at pH 5.5 (Desmoulin et al., 2010). At the end of the incubations, transport was quenched with ice-cold DPBS, cells were washed three times with ice-cold DPBS, and cellular proteins were solubilized with 0.5 N NaOH. Levels of drug uptake were expressed as pmoles per milligram of protein calculated from direct measurements of radioactivity (model LS6500 scintillation counter; Beckman Coulter, Fullerton, CA) and protein content (Folin-phenol reagent) of cell homogenates.

The whole-cell Michaelis constant (K_t) and maximal velocity (V_{max}) for [^{3}H]L-AMT, [^{3}H]D-AMT, and [^{3}H]PMX transport by PCFT were determined by measuring transport rates in R2/hPCFT4 cells at pH 5.5, using substrate concentrations from 0.04 to 5.0 μM as described previously (Desmoulin et al., 2010). Rates were corrected for the passive transport rate in R2 cells under the same conditions and concentrations. K_t and V_{max} values were determined from Lineweaver-Burke plots.

Competition of [^{3}H]L-AMT (0.5 μM) uptake was measured over 2 min at 37°C in R2/hPCFT4 cells at pH 5.5, 6.5, and 6.8 by unlabeled L-AMT (10 μM), D-AMT (10 or 30 μM), PMX (10 μM; IC_{50} = 13.2 nM for R2/hPCFT4 cell growth), and compound 1 (10 μM; IC_{50} = 43.4 nM for R2/hPCFT4 cell growth) (Wang et al., 2010; Kugel Desmoulin et al., 2011). Levels of [^{3}H]L-AMT uptake were measured as described above.

LC-MS/MS Analysis of Plasma L-AMT and D-AMT

Total AMT in dog and human plasma (i.e., L-and D-enantiomers) was quantitated by achiral LC-MS/MS using a method for each species (representative details below). The percentage of L-and D-enantiomer in the plasma of either species was determined by LC-MS/MS using a chiral stationary phase.

Achiral Quantitation of Total L-AMT and D-AMT in Dog Plasma. Quantitation of total AMT in dog plasma (i.e., L- and D-enantiomers) was conducted by achiral LC-MS/MS using a API 3000 tandem mass spectrometer (Applied Biosystems/MDS Sciex, Foster City, CA) equipped with a high-performance liquid chromatograph (Agilent 1200; Agilent Technologies, Santa Clara, CA). Analyst 1.4.2 software (Applied Biosystems/MDS Sciex) was used to control the system, quantify peak areas, perform linear regression analysis, and calculate sample concentrations.

A 100-μl aliquot of plasma was mixed with 200 μl of acetonitrile (Sigma) containing 10 ng of the internal deuterated standard LD-AMT-d_3. After vortex mixing for 1 min, the sample was centrifuged at 7000 rpm at 4°C for 10 min to pellet precipitated proteins. The supernatant was transferred to an amber 2-ml polypropylene high-performance liquid chromatography vial (SUN-SRi, Rockwood, TN), diluted with 700 μl of water, and vortex-mixed before analysis by LC-MS/MS.

Freshly prepared L/D-AMT standard curves were analyzed along with samples on each day of analysis. Instrument calibrators and quality-control (QC) samples were prepared by adding 10 μl of a stock L/D-AMT solution (in a methanol/water mixture, v/v 50:50) to 100 μl of dog plasma (Bioreclamation Inc., Westbury, NY). Calibrator concentrations were 1, 2, 5, 10, 50, 100, 500, and 1000 ng/ml. QC samples were prepared at approximately 2.4, 400, and 800 ng/ml. Calibrators and QC samples were processed for analysis using the procedure described above.

A 20-μl sample was injected onto a Kinetex pentafluorophenyl-phase column (50 × 2.1 mm, 2.6 μ, 100 Å; Phenomenex, Torrance, CA) maintained at 40°C and eluted by a mobile phase with initial conditions of 80% solvent A for 0.5 min, followed by a step gradient to 5% solvent A held for 5 min (solvent A, 0.1% formic acid in water; solvent B, 0.1% formic acid in methanol), followed by an immediate return to initial conditions maintained for 3 min, at a flow rate of 0.3 ml/min. The typical retention time for L-and D-enantiomers and internal standard was 1.6 min with an assay-to-assay run time of 8 min.

A turbo ion spray interface was used as the ion source operating in positive ion mode. Acquisition was performed by using multiple reaction monitoring for the L-and D-AMT *m/z* transition 441.2 to 294.2 and the LD-AMT-d_3 *m/z* transition 444.2 to 294.2. Ion spray voltage was 3000 V; ion source temperature was 450°C; and collision energy was −35 V. Peak areas of the analyte and internal standard were quantified with Analyst 1.4.2 software (Applied Biosystems/MDS Sciex). The lower limit of quantification in dog plasma was reported as 1 ng/ml.

Achiral Quantitation of Total L-AMT and D-AMT in Human Plasma. Quantitation of total AMT in human plasma was conducted by achiral LC-MS/MS using a API 5500 triple quadrupole mass spectrometer (Applied Biosystems/MDS Sciex) equipped with a high-performance liquid chromatograph (Agilent 1200SL; Agilent Technologies), Analyst 1.5 software (Applied Biosystems/MDS Sciex), and a HTC PAL autosampler (CTC Analytics AG, Zwingen, Switzerland).

Deuterated internal LD-AMT-d_3 standard was prepared in deionized water at 40 ng/ml. Calibrators and QC samples were prepared by adding 10, 50, or 150 μl of stock L/D-AMT solutions (in 50:50 methanol/water) to 4.95 or 14.85 ml (QCs), or 0.990 ml (calibrators) of human plasma. QC samples were prepared at 0.2, 0.6, 3.0, 40.0, and 250 ng/ml. Calibrator concentrations were 0.2, 0.40, 1.0, 4.0, 10.0, 25.0, and 50.0 ng/ml. A 10-μl aliquot each of the calibrators and QCs was added to 0.390 ml of blank plasma, then processed as described below.

Subject plasma samples, calibrators, QCs, and blanks were processed by solid-phase extraction using an Oasis HLB 96-well plate (Waters, Milford, MA) on a Cerex 96 Pressure Processor μSPE processing system (Crawford Scientific Ltd., Lanarkshire, Scotland). To a 96-well plate was added a 100-μl aliquot of a subject sample and each of the above calibrators, QCs, and blanks, followed by 300 μl of 5:95 formic acid/water and 20 μl (0.8 ng) of the internal deuterated LD-AMT-d_3 standard. The plate was vortexed 1 min and centrifuged 2 min at 1200 rpm, and the entire volume of each well was transferred to a conditioned extraction block with a multichannel pipette. The extraction block was rinsed with 800 μl of water and 800 μl of 10:90 methanol/water (v/v). Analyte was eluted from the extraction block with 2 × 250 μl of methanol. The eluant was evaporated to dryness at 45°C and reconstituted with 100 μl of 0.1:10:90 (v/v/v) formic acid/methanol/water. The samples were vortex-mixed gently for 0.5 min, centrifuged for 2 min at 3200 rpm, and submitted to the autosampler.

A 10-μl sample was injected onto an ACE-C_{18} column (2.1 × 50 mm, 3.0 μ; Advanced Chromatography Technologies, Aberdeen, United Kingdom) and eluted by a mobile phase at a flow rate of 0.7 ml/min with initial conditions of 0% solvent B for 30 s, followed by a series of gradients: 0% solvent B to 60% solvent B over 150 s, 60% solvent B to 95% solvent B over 40 s, and 95% solvent B to 0% solvent B over 80 s [solvent A, 0.1:95:5 (v/v/v) formic acid/water/acetonitrile; solvent B, 0.1:50:50 (v/v/v) formic acid/acetonitrile/methanol]. Using the positive ionization mode, mass spectral analyses were performed by using multiple reaction monitoring for the AMT *m/z* transition of 441 to 294 and the LD-AMT-d_3 *m/z* transition of 444 to 294 (each a dwell time of 100 ms), with a source temperature of 550°C. The peak areas of the analyte and internal standard were quantified by using Analyst 1.5 (Applied Biosystems/MDS Sciex). The lower limit of quantitation was 0.2 ng/ml, and the linear range was 0.2 to 50.0 ng/ml ($R^2 > 0.99$).

Chiral Quantitation of Percentage of L-AMT and D-AMT in Plasma. The percentage of L- and D-enantiomers in dog or human plasma was determined by using the LC-MS/MS systems and sample preparation as described above, but equipped with a Chirobiotic T (teicoplanin) stationary-phase column (150 × 2 mm, 5 μm; Astec, Whippany, NJ) maintained at 40°C. The mobile phase consisted of 0.2% ammonium hydroxide and 0.4% acetic acid (v/v) in methanol. A constant mobile phase flow rate (0.2 ml/min) was provided, and the

L-and D-enantiomers were quantitated by using the mass spectral analyses described for the achiral assays above. The typical retention times for L- and D-enantiomers were 9.3 and 12.3 min, respectively. Peak areas for L- and D-enantiomers were determined and expressed as a percentage of total AMT.

Statistical Analyses

Statistical differences in the dog studies were determined by using the unpaired Student's *t* test. Differences were considered significant at $p < 0.05$. Statistical bioequivalence of L/D-AMT (test) and L-AMT (reference) in the phase 1 clinical trial was determined by computing the 90% confidence interval (CI) of the test-to-reference ratio for the natural log-transformed primary pharmacokinetic endpoints (i.e., AUC_{∞}, $AUC_{(0-12\ h)}$, and C_{max}) derived from plasma L-AMT (Balthasar, 1999). Bioequivalence was established if the 90% CI of the test-to-reference ratios for the primary pharmacokinetic endpoints were within 0.8 and 1.25. The target power of the trial was 85% assuming an intrasubject CV of 20%, test/reference of 0.95, and minimum sample size of 22 (Rani, 2007). The statistical analysis for bioequivalence requires that a subject provide primary pharmacokinetic endpoints for both test and reference. Thus the statistical plan specified that subjects who provided ≥90% of all planned samples were included in the bioequivalence analysis. The primary safety endpoints in the phase 1 clinical trial were the incidence of adverse events (AEs) and serious AEs (SAEs). Other safety endpoints included incidences of drug-related AEs and SAEs, AEs by severity, study drug discontinuations, and deaths. Statistical differences in the incidence of safety endpoints were determined by using Fisher's exact test. All subjects administered AMT were included in the safety analyses. Pearson's correlation examined the significance between pharmacokinetics and subject variables (e.g., dose and GFR). Statistical differences in mean pharmacokinetic parameters in subjects without and with AEs were determined by using the unpaired Student's *t* test. All analyses in the phase 1 clinical trial, except the bioequivalence analysis, were two-tailed using a *p* value of 0.05.

Pharmacokinetic Calculations

Concentration-time profiles were analyzed by using standard noncompartmental methods (PK Solutions Version 2.0 for Windows XP; Summit Research Service, Montrose, CO). Maximal concentration (C_{max}) and T_{max} were derived directly from the observed concentrations. The area associated with the concentration-time profile from 0 h to the last time with a quantifiable concentration (C_n) was derived by using the linear-trapezoidal method (i.e., $AUC_{(0-4\ h)}$ or $AUC_{(0-12\ h)}$). The method of residuals was used to resolve the concentration-time profile curve into three exponential terms corresponding to absorption, distribution, and terminal elimination phases based on the assumption that each disposition phase was an apparent first-order rate process. Using the method of residuals, the three linear portions of a semilog plot of each concentration-time curve were estimated starting with the terminal elimination phase. Each linear portion was subjected to linear regression to establish the rate constants of each exponential term, including the apparent terminal rate constant λ_z. The apparent terminal elimination phase half-life ($t_{1/2}$) was calculated as $\ln(2)/\lambda_z$. For pharmacokinetic collections lasting 12 h, the area associated with the concentration-time profile from 0 h to infinity (AUC_{∞}) was computed as $AUC_{(0-12\ h)} + (C_n/\lambda_z)$. Apparent total body clearance (CL) was computed as D/AUC_{∞}, where *D* is the dose of the L-enantiomer. The apparent volume of distribution (V_D) was computed as CL/λ_z. CL and V_D were normalized to body weight and are presented as CL/kg and V_D/kg, respectively. Human GFR was determined from the creatinine clearance calculated from serum creatinine concentration, sex, age, and body weight by using the formula developed by Cockcroft and Gault (1976). GFR in the beagle dog was set to the mean (95% CI) renal inulin clearance established from a weighted means analysis in healthy dogs (Von Hendy-Willson and Pressler, 2011). The CV of a pharmacokinetic parameter was computed as the S.D./mean. Intrasubject and intersubject variability (CV) of a pharmacokinetic parameter was calculated as $CV = \sigma_e/\mu_R$, where σ_e is the residual mean square for intrasubject or intersubject error obtained from the analysis of variance, and μ_R is the mean of the reference study drug (Liu, 1991; Mohsen, 2010).

Results

Pharmacokinetics and Toxicity of L-AMT and D-AMT in Dogs

The oral pharmacokinetics and toxicity of L-AMT and D-AMT were evaluated in 40 beagle dogs in escalating doses (Fig. 2, A and B; Table 1). There was moderate variability in pharmacokinetic parameters among the dose groups (mean C_{max} CV for L-AMT and D-AMT of 0.21 and 0.46, respectively; mean $AUC_{(0-4\ h)}$ CV for L-AMT and D-AMT of 0.24 and 0.44, respectively). The C_{max} (Fig. 2C) and $AUC_{(0-4\ h)}$ (Fig. 2D) were dose proportional over the L-AMT dose range of 0.02 to 0.2 mg/kg and the entire tested D-AMT dose range of 0.8 to 82.5 mg/kg. The C_{max} of L-AMT was 11- and 6-fold larger than the C_{max} of D-AMT at doses of 0.8 and 2.5 mg/kg, respectively (Fig. 2C; $p < 0.001$). The $AUC_{(0-4\ h)}$ of L-AMT was 12- and 6-fold larger than the $AUC_{(0-4\ h)}$ of D-AMT at doses of 0.8 and 2.5 mg/kg, respectively (Fig. 2D; $p < 0.001$). There was no dose-dependent trend in T_{max} for either L-AMT or D-AMT and no significant difference between the T_{max} values for L-AMT and D-AMT (Table 1). Both nonlinearity in C_{max} and $AUC_{(0-4\ h)}$ at L-AMT doses above 0.2 mg/kg and stereoselectivity in C_{max} and $AUC_{(0-4\ h)}$ for L-AMT over D-AMT suggest that absorption involved a transporter-mediated component.

The toxicity of L-AMT and D-AMT was evaluated in each of the 40 beagle dogs as a function of dose through detailed daily clinical and physical observations and terminal necropsy that included gross and histopathologic examinations (Table 1). An additional vehicle group of four beagle dogs served as a negative control (data not shown). Beginning 3 days after the oral administration of L-AMT, dogs in the 0.8 and 2.5 mg/kg dose groups exhibited severe lethargy, anorexia, vomiting, weight loss, and diarrhea (including bloody) characteristic of acute antifolate intoxication, with one dog found dead and another found moribund and then euthanized in the 2.5 mg/kg dose group. Dogs in the 0.2 mg/kg L-AMT dose group exhibited weight loss and diarrhea 5 days after dosing. Dogs in the remaining 0.02 and 0.08 mg/kg L-AMT dose groups exhibited no significant signs of clinical antifolate toxicity. At necropsy, dogs in the 2.5 mg/kg L-AMT dose group were found to have multiple red and pigmented lesions throughout the small and large intestines. Histologic changes in the L-AMT dose groups consisted of epithelial necrosis and neutrophilic inflammation in the duodenum and jejunum (2.5 and 0.8 mg/kg) and mild to moderate bone marrow hypocellularity (2.5, 0.8, and 0.2 mg/kg). Dogs in the remaining L-AMT dose groups had no significant gross lesions or histopathologic findings at necropsy. Although the largest D-AMT dose (82.5 mg/kg) was 100-fold greater than the maximal nonlethal L-AMT dose (0.8 mg/kg) and yielded a 7-fold greater exposure in the plasma, none of the D-AMT dose groups exhibited any signs of clinical toxicity, and there were no significant gross lesions or histopathologic changes at necropsy (Table 1).

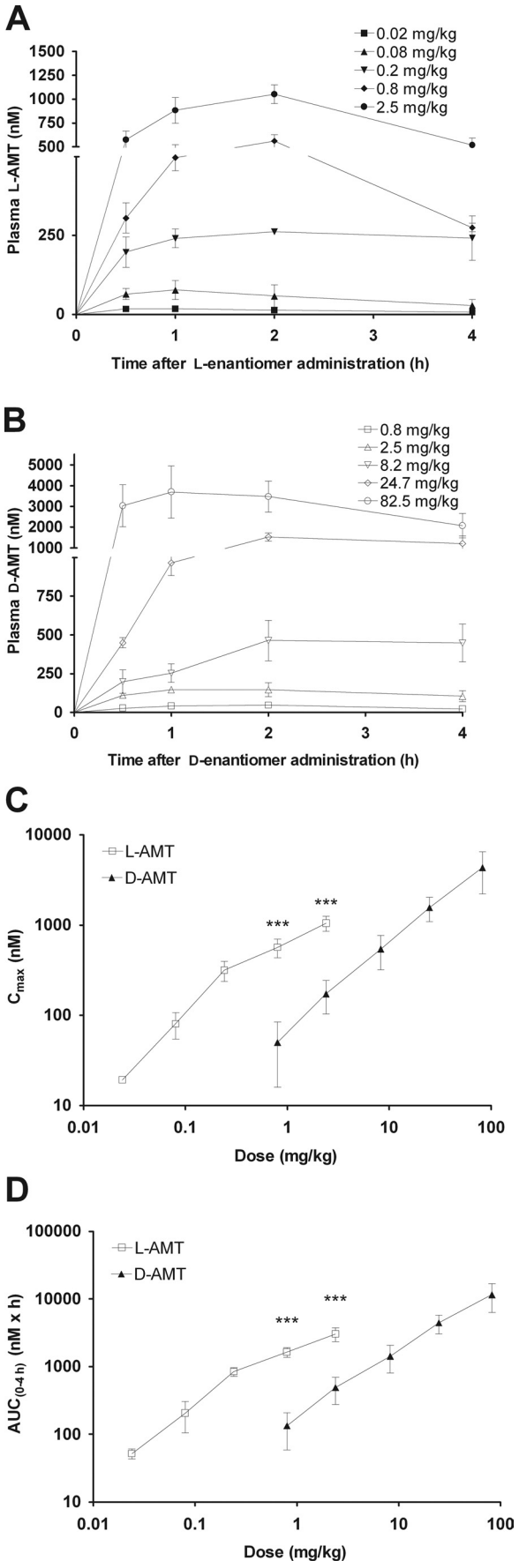

Pharmacokinetics of L-AMT and L/D-AMT in Dogs

The oral pharmacokinetics of L-AMT and L/D-AMT were evaluated in 10 beagle dogs at the same dose of L-enantiomer in a randomized, single-dose, two-way crossover design (Fig. 3; Table 2). There was no detectable D-enantiomer in plasma after dosing either L-AMT or L/D-AMT (data not shown), ruling out in vivo racemization and suggesting a stereoselective transporter-mediated component in absorption. Pharmacokinetic parameters therefore were derived for plasma L-enantiomer only. Peak plasma concentrations of L-AMT and L/D-AMT (90 ± 50 and 100 ± 50 nM) were achieved after 1 h (1.1 ± 0.5 and 1.0 ± 0.5 h) and declined with a terminal half-life of 2 to 3 h (3.0 ± 1.5 and 2.1 ± 0.4 h) to approximately 30-fold lower levels (2.7 ± 4.9 and 4.4 ± 6.6 nM) by 12 h. The CV in the primary pharmacokinetic parameters was similar for L-AMT and L/D-AMT: C_{max}, 0.55 versus 0.50; $AUC_{(0-12\ h)}$, 0.52 versus 0.55; AUC_{∞}, 0.48 versus 0.53); T_{max}, 0.45 versus 0.50; and $t_{1/2}$, 0.50 versus 0.19. The overall clearance of L-AMT and L/D-AMT was 3- and 2-fold over GFR, respectively. There was no significant difference between the mean pharmacokinetic parameters for L-AMT and L/D-AMT ($p > 0.05$). These results suggest the D-enantiomer in L/D-AMT did not influence the absorption or disposition of the L-enantiomer in the dog.

Phase 1 Pharmacokinetic and Bioequivalence Trial of L-AMT and L/D-AMT In Humans with Psoriasis

Given that there was no significant difference between the mean pharmacokinetic parameters for L-AMT and L/D-AMT in dogs, we conducted a formal phase 1 bioequivalence study of L-AMT and L/D-AMT in human subjects with psoriasis to determine whether the D-enantiomer in L/D-AMT influenced L-enantiomer pharmacokinetics in humans. The trial was also a first in-human administration of the D-enantiomer, thus potential differences in the safety of L-AMT and L/D-AMT were assessed.

Subjects. Twenty-four subjects were screened and 22 subjects (19 white, 1 Hispanic, 2 African American) aged 22 to 58 (42 ± 9.8 years) were randomized (Table 3). The 22 randomized subjects weighed 52 to 129 kg (81 ± 19 kg) with a body mass index of 19 to 39 (29 ± 6.1). Two subjects were screened, but not randomized, one subject withdrew consent, and one subject had an abnormal screening lab. All 22 randomized subjects were included in the safety assessments. Two randomized subjects did not complete the study per protocol: subject 115 missed the 10- and 12-h blood collections on study day 7, and subject 119 did not attend study day 7. Per protocol, subject 119 was withdrawn from the bioequivalence statistical analyses (see *Materials and Methods*).

Fig. 2. Dog pharmacokinetics after the single-dose oral administration of L-AMT and D-AMT. Ten groups of four animals each received a single 2-ml oral dose of L-AMT or D-AMT solution in an escalating fashion from 0.02 to 2.5 mg/kg for the L-enantiomer and 0.8 to 82.5 mg/kg for the D-enantiomer. Blood samples were taken at specified intervals over 4 h after dosing. Concentrations of the L-and D-enantiomers in plasma were quantitated by using LC-MS/MS. Pharmacokinetic parameters C_{max} and $AUC_{(0-4\ h)}$ were calculated as described in the *Materials and Methods*. Values are mean ± S.D. ($n = 4$ per dose). A, concentration-time profiles after L-AMT dosing. B, concentration-time profiles after D-AMT dosing. C, change in C_{max} as a function of increasing dose. D, change in $AUC_{(0-4\ h)}$ as a function of increasing dose. At the same dose (0.8 and 2.5 mg/kg), the C_{max} and $AUC_{(0-4\ h)}$ of the L-enantiomer were significantly larger than the D-enantiomer. ***, $p < 0.001$.

TABLE 1

Mean (± S.D.) pharmacokinetic parameters and toxicity of L-AMT and D-AMT in dogs after oral administration of escalating doses of each enantiomer

L-AMT and L/D-AMT were orally administered separately to 40 beagle dogs (n = 4 per dose group) as described under *Materials and Methods*. Plasma samples were collected over a 4-h period and analyzed by LC-MS/MS. Pharmacokinetic parameters were derived from concentration vs. time profiles. Toxicity was determined as described under *Materials and Methods*.

Enantiomer	Dose	C_{max}	$AUC_{(0–4\ h)}$	T_{max}	Toxicity
	mg/kg	*nM*	*nM × h*	*h*	
L	0.02	19.2 ± 1.1	51.5 ± 9.1	0.6 ± 0.3	None
L	0.08	80.8 ± 26	206 ± 100	0.9 ± 0.3	None
L	0.2	316 ± 79	845 ± 124	2.3 ± 1.3	+
L	0.8	566 ± 130	1640 ± 264	1.8 ± 0.5	++++
L	2.5	1050 ± 198	3050 ± 721	2.0 ± 0.0	++++
D	0.8	50.0 ± 34	134 ± 75	1.4 ± 0.8	None
D	2.5	174 ± 70	488 ± 214	2.5 ± 1.0	None
D	8.2	543 ± 222	1430 ± 627	3.0 ± 1.2	None
D	24.7	1560 ± 465	4450 ± 1364	1.3 ± 0.5	None
D	82.5	4350 ± 2145	11,600 ± 5253	2.0 ± 1.4	None

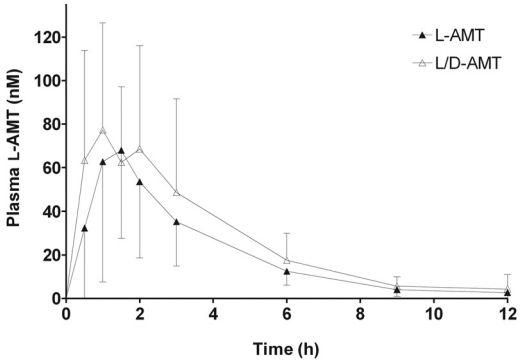

Fig. 3. Dog pharmacokinetics after the single-dose oral administration of L-AMT and L/D-AMT. Ten beagle dogs received L-AMT (0.77 mg of L-enantiomer) and L/D-AMT (0.7 mg of L-enantiomer and 0.3 mg of D-enantiomer) by gavage in a randomized, single-dose, two-way crossover design. Plasma samples were collected over a 12-h period and analyzed by LC-MS/MS as described under *Materials and Methods*. Pharmacokinetic parameters were derived from the concentration versus time profiles. There was no detectable D-enantiomer in the plasma after dosing of either drug product; values shown are only for the L-enantiomer in plasma. Shown are the mean plasma concentration-time profiles for L-AMT and L/D-AMT, where each concentration value is the mean ± S.D. There was no significant difference between L-AMT and L/D-AMT for any mean pharmacokinetic parameter ($p > 0.05$).

TABLE 2

Pharmacokinetic parameters of L-AMT and L/D-AMT in dogs given the same L-enantiomer dose

L-AMT and L/D-AMT were orally administered to 10 beagle dogs as described under *Materials and Methods*. Plasma samples were collected over a 12-h period and analyzed by LC-MS/MS. Pharmacokinetic parameters were derived from concentration vs. time profiles. There was no detectable D-enantiomer in the plasma after dosing of either drug product; values shown are only for the L-enantiomer in plasma. Values are mean ± S.D., n = 10 except for GFR/kg, which is the weighted mean (95% CI) as described under *Materials and Methods*. There was no significant difference between L-AMT and L/D-AMT for any mean pharmacokinetic parameter ($p > 0.05$).

	L-AMT	L/D-AMT
L dose, mg/kg	0.07 ± 0.01	0.06 ± 0.01
D dose, mg/kg		0.03 ± 0.004
C_{max}, nM	90 ± 50	100 ± 50
$AUC_{(0–12\ h)}$, nM × h	250 ± 130	330 ± 180
AUC_{∞}, nM × h	270 ± 130	340 ± 180
T_{max}, h	1.1 ± 0.5	1.0 ± 0.5
$t_{1/2}$, h	3.0 ± 1.5	2.1 ± 0.4
CL/kg, l/h/kg	0.80 ± 0.57	0.54 ± 0.31
GFR/kg, l/h/kg	0.24 (0.21–0.26)	0.24 (0.21–0.26)
V_D/kg, l/kg	4.2 ± 5.7	1.7 ± 1.0

Pharmacokinetics and Bioequivalence. The oral pharmacokinetics and bioequivalence of L-AMT and L/D-AMT at the same dose of L-enantiomer were evaluated in 22 subjects with moderate to severe psoriasis in a two-arm randomized, open-label, two-period crossover trial (Fig. 4; Table 4). As was the case in the dog, there was no detectable D-enantiomer in plasma after dosing either L-AMT or L/D-AMT (data not shown), ruling out in vivo racemization and suggesting a stereoselective component in absorption. Pharmacokinetic parameters were derived for plasma L-enantiomer only. C_{max}, $AUC_{(0–12\ h)}$, AUC_{∞}, T_{max}, and $t_{1/2}$ in the human were similar to those found in the dog given a 7-fold larger L-enantiomer dose. Peak plasma concentrations of L-AMT and L/D-AMT (74 ± 29 and 73 ± 28 nM, respectively) were achieved after approximately 1 h (1.12 ± 0.63 and 0.81 ± 0.30 h, respectively) and declined with a terminal half-life of 3.7 h (3.7 ± 0.8 and 3.7 ± 0.8 h, respectively) to approximately 25-fold lower levels (3.2 ± 1.7 and 2.6 ± 0.9 nM, respectively) by 12 h. The CV in the primary pharmacokinetic parameters was similar for L-AMT and L/D-AMT: C_{max}, 0.39 versus 0.38; $AUC_{(0–12\ h)}$, 0.32 versus 0.28; AUC_{∞}, 0.32 versus 0.28; T_{max}, 0.56 versus 0.37; and $t_{1/2}$, 0.22 versus 0.22. The intrasubject variability was less than the intersubject variability for both C_{max} (22 versus 50%; Fig. 4B) and AUC_{∞} (11 versus 39%; Fig. 4C). There was a significant linear correlation (Fig. 5) between individual subject values for C_{max} versus dose (L-AMT, $p = 0.002$; L/D-AMT, $p = 0.001$), AUC_{∞} versus dose (L-AMT, $p = 0.0002$; L/D-AMT, $p = 0.003$), and AUC_{∞} versus GFR (L-AMT, $p = 0.02$; L/D-AMT, $p = 0.001$). The ratio of the

TABLE 3

Baseline demographics of human subjects with psoriasis enrolled in the phase 1 trial

Baseline Demographic sex	n = 22
Male	8 (36.4%)
Female	14 (63.6%)
Race/ethnicity	
White	19 (86.4%)
Hispanic	1 (4.5%)
African American	2 (9.1%)
Age at study entry, years	
Mean ± S.D.	42 ± 9.8
Median	42
Range	22–58
Weight at study entry, kg	
Mean ± S.D.	81 ± 19
Median	81
Range	52–129
Body mass index at study entry, kg	
Mean ± S.D.	29 ± 6.1
Median	28
Range	19–39

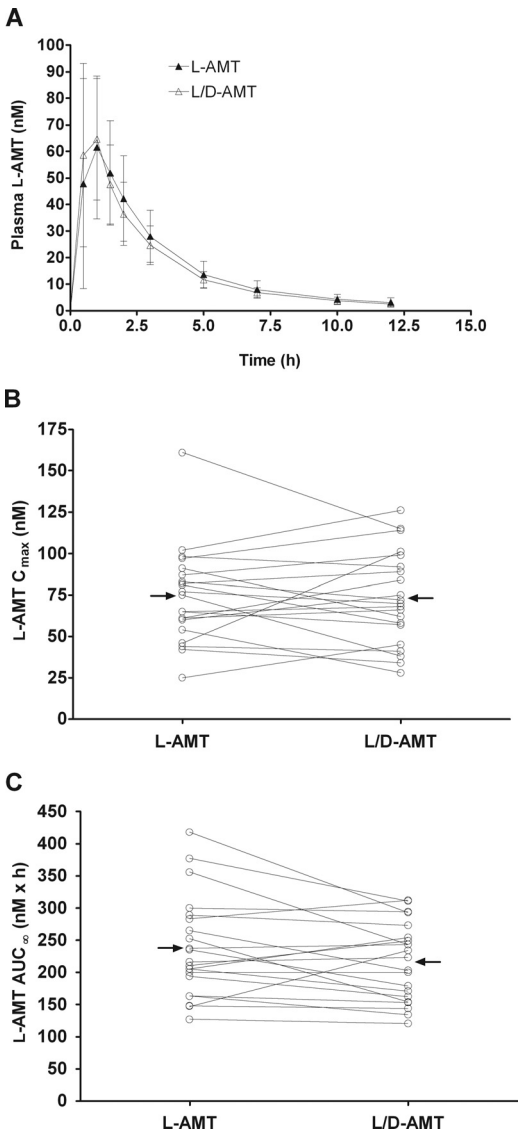

Fig. 4. Bioequivalence of L-AMT and L/D-AMT in psoriatic subjects (n = 21) after single-dose oral administration of L-AMT (0.7 mg of L-enantiomer) and L/D-AMT (0.7 mg of L-enantiomer and 0.3 mg of D-enantiomer) in a phase 1, two-arm randomized, open-label, two-period crossover trial. Plasma samples were collected over a 12-h period and analyzed by LC-MS/MS as described under *Materials and Methods*. Pharmacokinetic parameters were derived from concentration versus time profiles. There was no detectable D-enantiomer in the plasma after dosing of either drug product; values shown are only for the L-enantiomer in plasma. A, plasma concentration-time profiles for L-AMT and L/D-AMT, where each concentration value shown is the mean ± S.D. B and C, the pharmacokinetic parameters C_{max} (B) and AUC_{∞} (C) derived for plasma L-AMT are shown as a function of administered L-AMT and L/D-AMT. Lines connect data points for the same subject, and horizontal arrows point to the group mean. The C_{max} and AUC_{∞} for L-AMT and L/D-AMT were bioequivalent (i.e., the 90% CI of the C_{max} and AUC_{∞} ratios for L-AMT and L/D-AMT within 0.8–1.25).

overall clearance to GFR was close to 1 for both L-AMT and L/D-AMT (Table 4), and the weight normalized clearance (CL/kg) was 6- to 9-fold smaller in the human than in the dog. L-AMT was bioequivalent to L/D-AMT (Table 4; 90% CI values between 0.8 and 1.25 for C_{max}, $AUC_{(0-12\ h)}$, and AUC_{∞}). These results suggest the D-enantiomer in L/D-AMT did not influence the absorption or disposition of the L-enantiomer in the human.

TABLE 4

Pharmacokinetic parameters and bioequivalence of L-AMT and L/D-AMT in humans with psoriasis given the same L-enantiomer dose

L-AMT and L/D-AMT were orally administered to 21 human subjects with psoriasis as described under *Materials and Methods*. Plasma samples were collected over a 12-h period and analyzed by LC-MS/MS. Pharmacokinetic parameters were derived from concentration vs. time profiles. There was no detectable D-isomer in the plasma after dosing of either drug product; values shown are only for the L-isomer in plasma. L-AMT was bioequivalent to L/D-AMT (i.e., 90% CI value between 0.8 and 1.25 for C_{max}, $AUC_{(0-12\ h)}$, and AUC_{∞}). Values are mean ± S.D. (n = 21).

	L-AMT	L/D-AMT	90% CI of the Ratio
L dose, mg/kg	0.01 ± 0.002	0.01 ± 0.002	
D dose, mg/kg		0.004 ± 0.001	
C_{max}, nM	74 ± 29	73 ± 28	0.82–1.07
$AUC_{(0-12\ h)}$, nM × h	218 ± 70	202 ± 57	0.84–0.98
AUC_{∞}, nM × h	238 ± 78	217 ± 61	0.82–0.97
T_{max}, h	1.12 ± 0.63	0.81 ± 0.30	
$t_{1/2}$, h	3.7 ± 0.8	3.7 ± 0.8	
CL/kg, l/h/kg	0.093 ± 0.026	0.099 ± 0.025	
GFR/kg, l/h/kg	0.094 ± 0.021	0.094 ± 0.021	
V_D/kg, l/kg	0.48 ± 0.13	0.52 ± 0.15	

Safety. Thirteen subjects (59.1%) reported 27 clinical AEs. There was no significant difference between the incidence of one or more AEs in the 7 days after the administration of L-AMT (50%) or L/D-AMT (43%). Overall, there were no AEs greater than grade 2, no SAEs, and no AEs that limited study drug administration. Severity grades 1 and 2 comprised 78 and 22% of all clinical AEs, respectively. AEs in the "general disorder" category were the most common (22%), and the spectrum of AEs after administration of L-AMT and L/D-AMT was similar. Fifteen AEs reported by eight subjects were judged related to study drug (drug-related AEs). Nine drug-related AEs (in seven subjects) occurred during the 7 days after L-AMT, whereas six drug-related AEs (in four subjects) occurred during the 7 days after L/D-AMT. Of the drug-related AEs, five (33%) were fatigue; four (27%) were nausea or vomiting; and three (20%) were headaches. All drug-related AEs were grade 1, except one grade 2 photophobia AE. There was no significant difference in the systemic exposure of the L-enantiomer in subjects with (+AE) and without (−AE) drug-related AEs (Fig. 6). There was no significant difference in body weight or GFR in subjects with (+AE) and without (−AE) drug-related AEs (data not shown). There were 16 grade 1 safety lab AEs. There was no significant difference in the incidence or magnitude of safety lab AEs obtained at baseline and 7 days after L-AMT or L/D-AMT dosing.

In Vitro Transport of L-and D-AMT by the Human PCFT

Membrane transport of D-and L-AMT enantiomers by PCFT was examined in R2/hPCFT4 CHO cells engineered to express the human transporter. R2/hPCFT4 cells were incubated with [^{3}H]D-AMT or [^{3}H]L-AMT (both at 0.5 μM) for different times and at pHs including those that characterize the upper intestine where dietary folate and antifolates are absorbed (Zhao et al., 2009, 2011). At pH 5.5, transport of [^{3}H]L-AMT and [^{3}H]D-AMT by PCFT was linear from 1 to 5 min, although cellular uptake of [^{3}H]L-AMT exceeded that for [^{3}H]D-AMT by 20- to 30-fold (Fig. 7A). Transport of both L-and D-AMT was nominal in transporter-null R2 cells at pH 5.5. At pH 6.5 and 6.8, PCFT transport of [^{3}H]L-AMT was still significant but was substantially reduced from that at pH 5.5 (~91 and ~95%, respectively, over the nominal level in R2 cells) (Fig. 7, B and C). Analogous results were observed with PMX, an antifolate structurally similar to AMT and an ex-

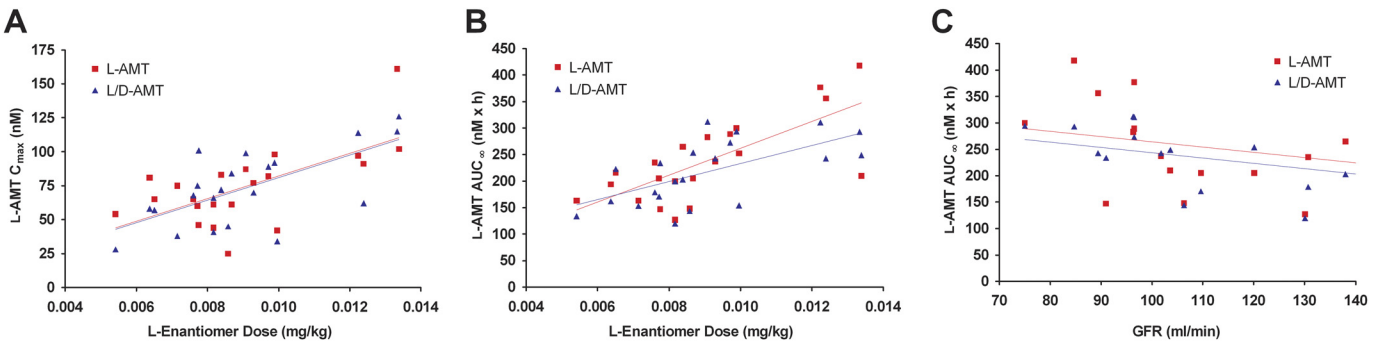

Fig. 5. Comparison of L-AMT and L/D-AMT pharmacokinetic parameters in subjects with psoriasis (n = 21) against dose (of the L-enantiomer) and GFR. A, C_{max} versus dose. B, AUC_∞ versus dose. C, AUC_∞ versus GFR. There was a significant linear correlation for C_{max} versus dose (L-AMT, p = 0.002; L/D-AMT, p = 0.001), AUC_∞ versus dose (L-AMT, p = 0.0002; L/D-AMT, p = 0.003), and AUC_∞ versus GFR (L-AMT, p = 0.02; L/D-AMT, p = 0.001).

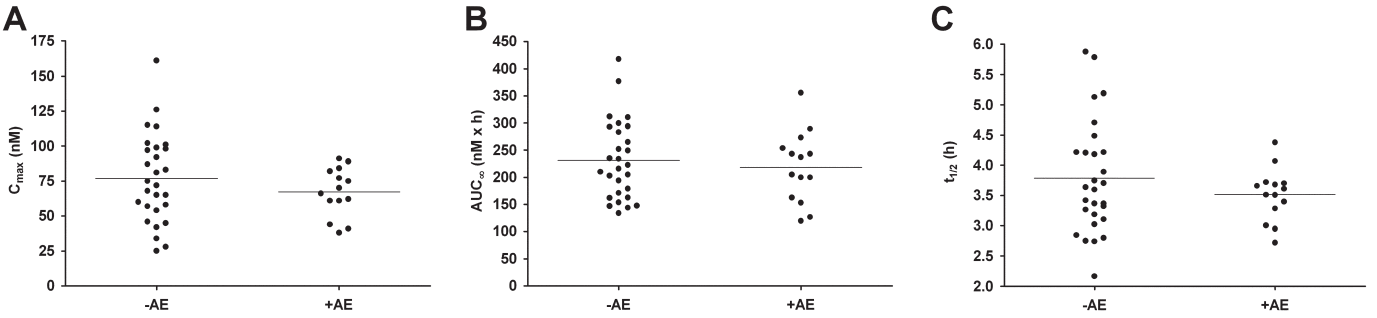

Fig. 6. Comparison of pooled L-AMT and L/D-AMT pharmacokinetic parameters (n = 42) in psoriatic subjects with no AEs (−AE) versus psoriatic subjects with at least one AE (+AE). A, C_{max} versus AE. B, AUC_∞ versus AE. C, $t_{1/2}$ versus AE. Horizontal bars are the mean. There was no significant difference between the means in the −AE and +AE groups for either C_{max}, AUC_∞, or $t_{1/2}$ ($p > 0.05$).

cellent substrate for PCFT transport (Fig. 7D). For [^{3}H]D-AMT at pH 6.5 and 6.8, drug uptake was not appreciably different from the residual level measured in R2 cells, indicating that D-AMT is not significantly transported by PCFT under these conditions.

Transport kinetics for PCFT were measured at pH 5.5 by using a range of concentrations of radioactive L-AMT, D-AMT, and PMX. Results were analyzed by Lineweaver-Burk plots and kinetic constants (K_t, V_{max}) for PCFT transport calculated (Table 5). Constants were compared with those previously reported for MTX in R2/hPCFT4 cells (Desmoulin et al., 2010). The results establish that at pH 5.5 V_{max} values, representing the maximal transport velocities, are modestly different between L-MTX, L-AMT, D-AMT, and PMX. Conversely, there were dramatic differences in the K_t values for these substrates, most prominently a 22-fold difference between L-AMT and D-AMT. PMX, the best transport substrate for PCFT yet described, displayed a K_t approximately 2.7-fold lower than that for L-AMT. Impressively, the V_{max}/K_t values, reflecting the overall efficiency of PCFT transport, differed by 35-fold between L-and D-AMT and 2.3-fold between L-AMT and PMX. Collectively, these results demonstrate the stereospecific transport of AMT by PCFT at pH 5.5, which is attributable almost entirely to markedly decreased binding affinity, as reflected in the K_t.

Although the studies in Fig. 7 establish transport of D-AMT at pH 5.5 and little to none at pH 6.5 or 6.8, to assess the potential impact of D-AMT on transport of L-AMT by human PCFT, we measured competition for transport of [^{3}H]L-AMT (0.5 μM) over 2 min at 37°C in R2/hPCFT4 cells at pH 5.5, 6.5, and 6.8 by unlabeled L-AMT (10 μM) and D-AMT (10 μM or 30 μM), compared with those by 10 μM PMX and 10 μM compound 1 (a PCFT-selective transport substrate) (Wang et al., 2010). The results demonstrate that at pH 5.5 L-AMT, but not D-AMT, binds effectively to human PCFT, as reflected by ~80% inhibition in the presence of 10 μM L-AMT (Fig. 8A). In contrast, 10 or 30 μM D-AMT were poorly inhibitory (~15 and ~26%, respectively) at pH 5.5. As expected, both PMX and compound 1 potently inhibited [^{3}H]L-AMT transport to levels approximating the residual level in R2 cells. At pH 6.5 and 6.8, the net level of [^{3}H]L-AMT uptake was decreased but the qualitative pattern of inhibition was similar, with inhibition by D-AMT being insignificant (Fig. 8, B and C). These data establish that the presence of D-isomer in the D/L-AMT mixtures has minimal effect on PCFT transport and intestinal absorption of L-AMT.

Discussion

L/D-AMT is the result of a novel synthetic route developed for commercial-scale production of the L-enantiomer (Zebala, 2007). L/D-AMT entered phase 1 clinical development based on preclinical and clinical studies that suggested the L-enantiomer may offer improved efficacy and/or safety compared with MTX (Smith et al., 1996; Ratliff et al., 1998; Cole et al., 2005, 2006, 2009). The primary objectives of this study were to determine the safety, absorption, and pharmacokinetics of the L-and D-enantiomers in preclinical and clinical models, investigate whether the D-enantiomer perturbed L-enantiomer absorption, and provide evidence for a mechanism of intestinal absorption. This is the first report of L/D-AMT administered to human subjects to our knowledge.

Assessments of the pharmacokinetics of the L-and D-enantiomer were made in dogs in escalating oral doses. The L-

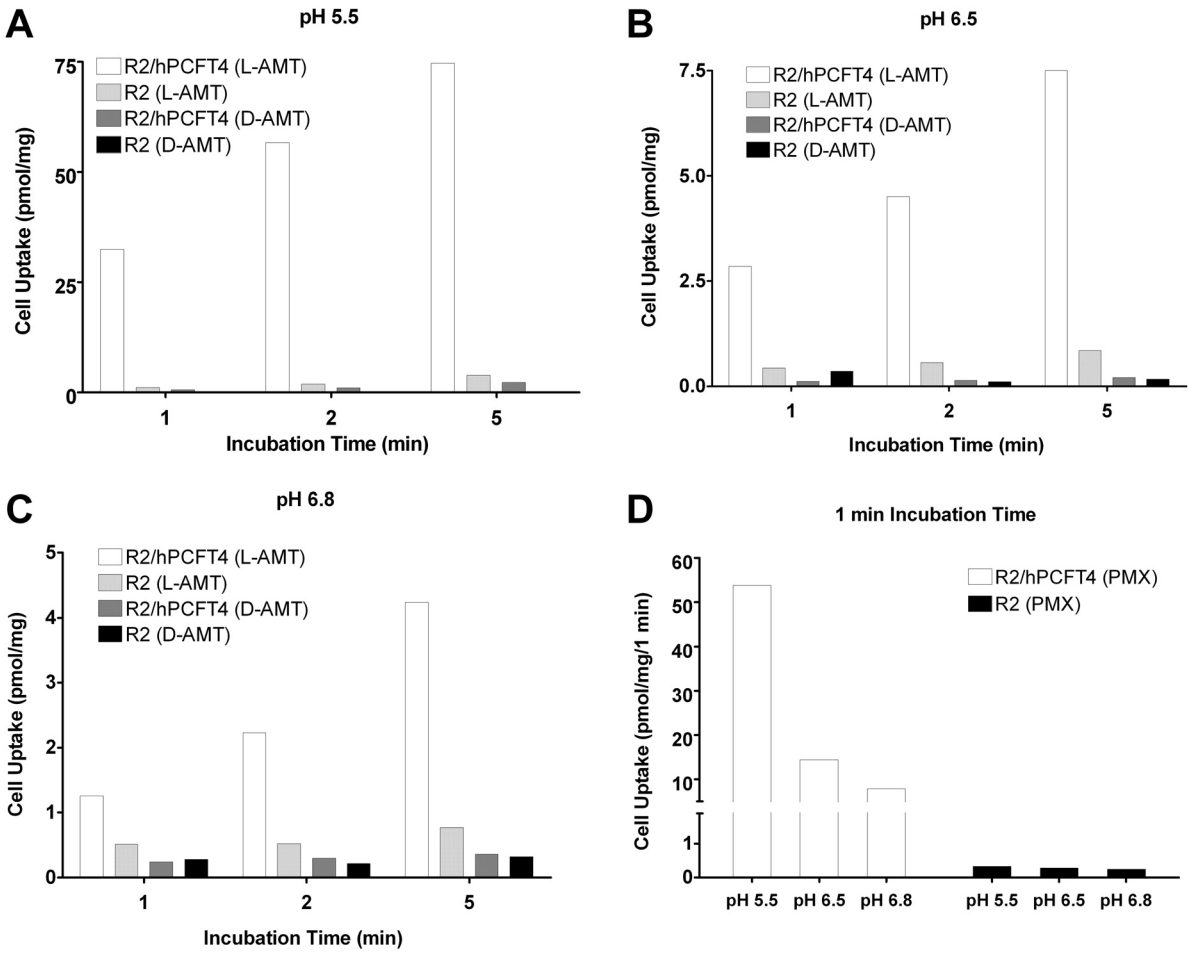

Fig. 7. Transport of L-AMT, D-AMT, and PMX by the human PFCT in vitro. A to C, CHO cells transfected with human PFCT (R2/hPCFT4 cells) or transporter-null R2 cells were incubated with 0.5 μM [^{3}H]L-AMT or [^{3}H]D-AMT at 37°C for 1, 2, and 5 min at pH 5.5 (A), pH 6.5 (B), or pH 6.8 (C). D, 0.5 μM [^{3}H]PMX was incubated with R2/hPCFT4 or transporter-null R2 cells at 37°C for 1 min at pH 5.5, 6.5, and 6.8. Data are the averages from duplicate experiments performed on the same day.

TABLE 5

Whole-cell kinetic constants of PCFT transport with antifolate substrates at pH 5.5

K_t and V_{max} were determined with the tritiated substrates [^{3}H]L-AMT, [^{3}H]D-AMT, [^{3}H]PMX, and [^{3}H]MTX in R2/hPCFT4 cells and calculated from Lineweaver Burke plots as described under *Materials and Methods*. L-MTX results were published previously (Wang et al., 2010). Values are mean values ± S.D. (n = 3).

Substrate	K_t	V_{max}	V_{max}/K_t
	μM	*pmol/mg/2 min*	*pmol/mg/2 min/μM*
D-AMT	15.0 ± 1.7	42.9 ± 13.0	2.8
L-AMT	0.69 ± 0.24	68.8 ± 18.5	99.7
PMX	0.26 ± 0.017	60.7 ± 8.9	233
L-MTX	0.28 ± 0.035	62.5 ± 14.9	223

enantiomer dose range was 0.02 to 2.4 mg/kg, and the D-enantiomer dose range was 0.8 to 82.5 mg/kg. Maximal plasma concentration and observed area under the curve were dose-proportional over the L-AMT dose range of 0.02 to 0.2 mg/kg and the entire tested D-AMT dose range of 0.8 to 82.5 mg/kg. The same pharmacokinetic parameters responded nonlinearly to L-AMT doses above 0.2 mg/kg. Identical doses of L-AMT and D-AMT produced stereoselective exposure to the L-enantiomer as reflected by a 6- to 12-fold larger maximal plasma concentration and observed area under the curve. Nonlinearity in pharmacokinetic parameters as a function of L-AMT dose and stereoselectivity for L-AMT over D-AMT together indicate a transporter-mediated component in absorption.

To investigate whether the D-enantiomer perturbed L-enantiomer absorption in dogs or humans, assessment of the pharmacokinetics of the L-enantiomer and L/D-enantiomer mixture were made at the same oral dose of the L-enantiomer. In dogs, there was no significant difference between the pharmacokinetic parameters obtained for plasma L-enantiomer after dosing of L-AMT or L/D-AMT. In humans, dosing of L-AMT and L/D-AMT resulted in bioequivalent L-enantiomer exposure in plasma. These results demonstrate that the D-enantiomer in L/D-AMT did not perturb the absorption or disposition of the L-enantiomer in dogs or humans.

There was no detectable plasma D-enantiomer after dosing either L-AMT or L/D-AMT in dogs and humans, indicating that L-AMT does not racemize in vivo and the absorption of L/D-AMT involves a stereoselective transporter. The absence of D-enantiomer in plasma after L/D-AMT dosing may be caused by in vivo competition by the L-enantiomer at the site of transporter-mediated uptake, because D-enantiomer was detected in dog plasma after D-AMT was administered alone (see in vitro PCFT competition discussion below).

L-AMT was not metabolized in vitro by human liver microsomes (data not shown), suggesting the compound is not significantly cleared by hepatic P450-dependent metabolism.

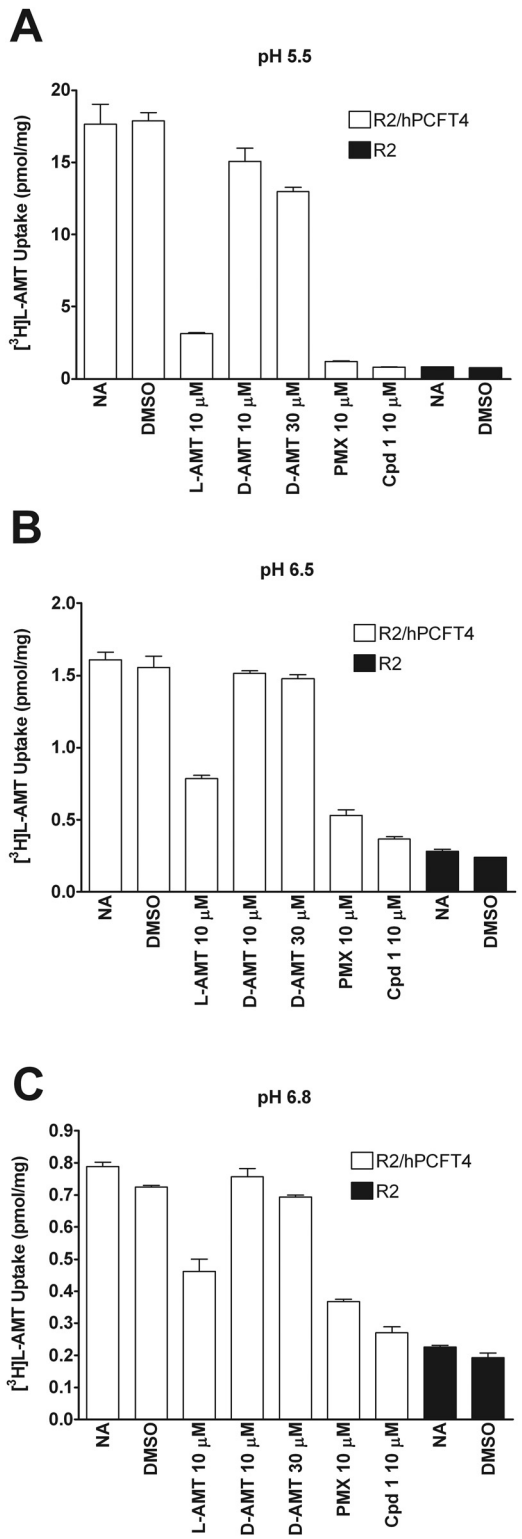

Fig. 8. Competition of L-AMT transport by the human PCFT. CHO cells transfected with human PFCT (R2/hPCFT4 cells) or transporter-null R2 cells were incubated with 0.5 μM [^{3}H]L-AMT at 37°C for 2 min at pH 5.5 (A), pH 6.5 (B), or pH 6.8 (C), and the transport of [^{3}H]L-AMT competed with 0.5% DMSO (vehicle for compound 1; Wang et al., 2010), 10 μM L-AMT, 10 or 30 μM D-AMT, 10 μM PMX, or 10 μM compound 1. A no-addition (NA) incubation served as a negative competition control. Values are averages ± S.D. (n = 4).

Consistent with renal elimination being the primary route of L-AMT excretion, 60% (median, range 19–78%) of an oral 6-mg L-AMT dose was found in the urine of human subjects (n = 9) collected over 72 h in a study that did not consider the dose fraction absorbed into the circulation (Swendseid et al., 1952). In the phase 1 human trial in this article, the ratio of total clearance to GFR was 0.99 and 1.05 for L-AMT and L/D-AMT, respectively. Taking into account an absorbed dose fraction less than 1, this suggests active tubular secretion may play a role in L-enantiomer elimination in the human as found previously for MTX (Liegler et al., 1969). Total weight-normalized clearance for L-AMT and L/D-AMT in dogs was 6- to 9-fold larger than in humans and 2- to 3-fold larger than the weight-normalized dog GFR. The mean ratio of renal MTX clearance to inulin clearance was 0.41 in dogs (n = 5) (Liegler et al., 1969). These results suggest species differences in the elimination of L-AMT and hepatic elimination of L-AMT may play a significantly larger role in the dog than in the human.

A previous report determined the pharmacokinetic parameters for the L-AMT tablet used in this study in 18 subjects with a median age of 15.5 years (range 3–18) with pediatric leukemia (Cole et al., 2008). The mean (± S.D.) pharmacokinetic parameters reported at a L-AMT dose of 0.06 mg/kg were C_{max} = 260 ± 85 nM, AUC_∞ = 1060 ± 297 nM × h, $t_{1/2}$ = 4.3 ± 2.0 h, and V_D/kg = 0.59 ± 0.38 l/kg. The median age of subjects with psoriasis in this study was 42 years (range 22–58), and the mean (± S.D.) pharmacokinetic parameters for L-AMT at a dose of 0.01 mg/kg were C_{max} = 74 ± 29 nM, AUC_∞ = 238 ± 78 nM × h, $t_{1/2}$ = 3.7 ± 0.8 h, and V_D/kg = 0.48 ± 0.13 l/kg. The above values are in close agreement with one another on a dose-adjusted basis, despite significant differences in age and disease background in the two patient populations. There is a minor downward variance in expected C_{max} (−41%) and AUC_∞ (−26%) at the 0.06 mg/kg dose based on dose proportionality of the same pharmacokinetic parameters at the 0.01 mg/kg dose. This may reflect partial saturation of the transporter-mediated uptake mechanism at the larger dose or greater clearance (e.g., renal) in the lower-aged group.

The maximal nonlethal L-AMT dose in the dog dose-escalation study presented in this report was 0.8 mg/kg, and it produced toxicity as described previously (Thiersch and Philips, 1949). Although the largest D-AMT dose (82.5 mg/kg) was 100-fold greater than the maximal nonlethal L-AMT dose and yielded a 7-fold greater plasma exposure, none of the D-AMT dose groups exhibited any signs of clinical toxicity, and there were no significant gross lesions or histopathologic changes at necropsy. Absent toxicity of the D-enantiomer may be caused by lower affinity to dihydrofolate reductase compared with the L-enantiomer and the inability of cells to retain the D-enantiomer via polyglutamation by folylpolyglutamate synthetase (McGuire et al., 1980; Cramer et al., 1984; Hendel and Brodthagen, 1984).

An assessment of human safety was undertaken in the phase 1 bioequivalence trial, which was a first in-human administration of the D-enantiomer. At an L-enantiomer dose predicted to provide optimal anti-inflammatory activity in future efficacy trials, there was no significant difference between the incidence of clinical or laboratory AEs in the 7 days after administration of L-AMT or L/D-AMT. Dosing of L-AMT or L/D-AMT was well tolerated. There were no AEs greater

than grade 2 (all drug-related AEs except one were grade 1), no SAEs, and no AEs that limited study drug administration. The most common drug-related AEs were fatigue, nausea or vomiting, and headache. Despite there being a significant linear correlation between individual subject values for C_{max} versus dose, AUC_{∞} versus dose, and AUC_{∞} versus GFR, subjects with and without drug-related AEs exhibited no significant differences in systemic exposure of the L-enantiomer, body weight, or GFR.

To elucidate the transporter potentially governing stereoselective uptake of the L-enantiomer over the D-enantiomer in dogs and humans, we conducted uptake and competition assays in vitro with cells engineered to express PCFT. The PCFT gene (SLC46A1) encodes a high-affinity, rheogenic, H^+-coupled folate transporter with high affinity (K_m = 1.5–3 μM at pH 6.5) for both oxidized folic acid and the naturally occurring reduced 5-methyltetrahydrofolate (Qiu et al., 2006). PCFT is highly expressed in the duodenum and proximal jejunum, the principal site of folate absorption, and is localized at the apical membrane (Qiu et al., 2007; Inoue et al., 2008). The PCFT involves a carrier-mediated process with a low-pH optimum that operates efficiently within the acidic microenvironment of the upper intestine, which has been reported to have a pH as low as 5.8 to 6.0 (Zhao et al., 2009, 2011). Mutations in PCFT cause the rare autosomal recessive disorder hereditary folate malabsorption (Qiu et al., 2006). In addition to dietary folates, PCFT transports some antifolate analogs (Qiu et al., 2006). Although previous studies in Caco-2 cells suggested that the reduced folate carrier (RFC1, SLC19A1) contributed to folate and folate analog absorption (Narawa et al., 2005, 2007), this view has since been revised (Narawa and Itoh, 2010). L-AMT is an excellent substrate for RFC, indeed better than MTX (Matherly et al., 1985). However, transport by RFC is optimal at neutral pH (Matherly et al., 2007) and decreases dramatically below pH 7 so that at pH 6.5 to 6.8, corresponding to the pH range found in the gut, transport is negligible even though RFC is present (as reflected by RFC transcripts) (Qiu et al., 2007). Conversely, PCFT has a pH optimum at 5.5 and transport is still significant at pH 6.5 to 6.8. PCFT was therefore likely to be key in determining the stereoselective intestinal absorption of L-AMT after oral dosage.

We demonstrated that at pH 5.5 PCFT transports D-AMT poorly compared with L-AMT, and at pH 6.5 or 6.8 the amount of D-AMT transported decreases to insignificant levels consistent with the low-pH optimum of the transporter. The kinetic constants (K_t, V_{max}) indicate that stereospecificity for the L-enantiomer over the D-enantiomer at pH 5.5 is attributable almost entirely to markedly decreased binding affinity rather than changes in transport rate. The V_{max}/K_t ratio for L-AMT, reflecting the overall efficiency of PCFT transport, was 35-fold greater than the ratio for D-AMT. Similar results have been reported for the in vitro transport of MTX enantiomers by PCFT (Narawa and Itoh, 2010).

Competition studies further demonstrated that independent of pH the D-enantiomer has no significant impact on PCFT transport of L-AMT even at concentrations up to 60 times higher than L-AMT. These results correlate with and explain the in vivo studies that demonstrate stereoselective uptake of L-AMT over D-AMT and bioequivalence of L-AMT and L/D-AMT. Stereoselective uptake of the L-enantiomer from L/D-AMT observed in vivo in dogs and humans thus most likely involves a mechanism of nearly complete exclusivity for PCFT transport and intestinal absorption of the L-enantiomer in the L/D-AMT mixture.

In conclusion, the clinical and preclinical evidence demonstrates a strong in vitro-in vivo correlation for the stereoselective absorption of orally administered L/D-AMT by PCFT, which mediates exclusion of the D-enantiomer from the systemic circulation in dogs and humans. Relative to L-AMT, the D-enantiomer in L/D-AMT did not perturb L-enantiomer absorption or alter the safety profile, resulting in L/D-AMT being bioequivalent to L-AMT. In our studies, both L/D-AMT and L-AMT were well tolerated at the putative anti-inflammatory dose investigated, and this initial evaluation will permit future testing of L/D-AMT as a potential therapeutic substitute for MTX in chronic inflammatory diseases that include psoriasis and rheumatoid arthritis.

Acknowledgments

We acknowledge the late Dr. Josiah Wedgwood of the National Institute of Allergy and Infectious Diseases/National Institutes of Health (Bethesda, MD) for his continued enthusiasm and support, without which the human clinical trial herein would not have been possible.

Authorship Contributions

Participated in research design: Menter, Cherian, Matherly, Kahn, and Zebala.

Conducted experiments: Menter, Thrash, Cherian, and Matherly.

Contributed new reagents or analytic tools: Wang, Gangjee, Morgan, Maeda, and Schuler.

Performed data analysis: Menter, Kahn, Cherian, Matherly, and Zebala.

Wrote or contributed to the writing of the manuscript: Menter, Matherly, Kahn, and Zebala.

References

Balthasar JP (1999) Bioequivalence and bioequivalency. *Am J Pharm Educ* **63:**194–198.

Cockcroft DW and Gault MH (1976) Prediction of creatinine clearance from serum creatinine. *Nephron* **16:**31–41.

Cole PD, Beckwith KA, Vijayanathan V, Roychowdhury S, Smith AK, and Kamen BA (2009) Folate homeostasis in cerebrospinal fluid during therapy for acute lymphoblastic leukemia. *Pediatr Neurol* **40:**34–41.

Cole PD, Drachtman RA, Masterson M, Smith AK, Glod J, Zebala JA, Lisi S, Drapala DA, and Kamen BA (2008) Phase 2B trial of aminopterin in multiagent therapy for children with newly diagnosed acute lymphoblastic leukemia. *Cancer Chemother Pharmacol* **62:**65–75.

Cole PD, Drachtman RA, Smith AK, Cate S, Larson RA, Hawkins DS, Holcenberg J, Kelly K, and Kamen BA (2005) Phase II trial of oral aminopterin for adults and children with refractory acute leukemia. *Clin Cancer Res* **11:**8089–8096.

Cole PD, Zebala JA, Alcaraz MJ, Smith AK, Tan J, and Kamen BA (2006) Pharmacodynamic properties of methotrexate and Aminotrexate during weekly therapy. *Cancer Chemother Pharmacol* **57:**826–834.

Cramer SM, Schornagel JH, Kalghatgi KK, Bertino JR, and Horváth C (1984) Occurrence and significance of D-methotrexate as a contaminant of commercial methotrexate. *Cancer Res* **44:**1843–1846.

Desmoulin SK, Wang Y, Wu J, Stout M, Hou Z, Fulterer A, Chang MH, Romero MF, Cherian C, Gangjee A, et al. (2010) Targeting the proton-coupled folate transporter for selective delivery of 6-substituted pyrrolo[2,3-*d*]pyrimidine antifolate inhibitors of de novo purine biosynthesis in the chemotherapy of solid tumors. *Mol Pharmacol* **78:**577–587.

Fiehn C (2009) The future of folic acid anatgonist therapy in rheumatoid arthritis. *Arthritis Rheum* **60:**1–4.

Flintoff WF and Nagainis CR (1983) Transport of methotrexate in Chinese hamster ovary cells: a mutant defective in methotrexate uptake and cell binding. *Arch Biochem Biophys* **223:**433–440.

Folsom JP, Miller AB, Bull H, Huff B, Wright WA, and McGilligan EF (1965) *Physicians' Desk Reference to Pharmaceutical Specialties and Biologicals*. Medical Economics, Inc., Oradell, NJ.

Hendel J and Brodthagen H (1984) Entero-hepatic cycling of methotrexate estimated by use of the D-isomer as a reference marker. *Eur J Clin Pharmacol* **26:**103–107.

Inoue K, Nakai Y, Ueda S, Kamigaso S, Ohta KY, Hatakeyama M, Hayashi Y, Otagiri M, and Yuasa H (2008) Functional characterization of PCFT/HCP1 as the molecular entity of the carrier-mediated intestinal folate transport system in the rat model. *Am J Physiol Gastrointest Liver Physiol* **294:**G660–G668.

Kugel Desmoulin S, Wang L, Hales E, Polin L, White K, Kushner J, Stout M, Hou Z,

Cherian C, Gangjee A, et al. (2011) Therapeutic targeting of a novel 6-substituted pyrrolo [2,3-*d*]pyrimidine thienoyl antifolate to human solid tumors based on selective uptake by the proton-coupled folate transporter. *Mol Pharmacol* **80:** 1096–1107.
Liegler DG, Henderson ES, Hahn MA, and Oliverio VT (1969) The effect of organic acids on renal clearance of methotrexate in man. *Clin Pharmacol Ther* **10:**849–857.
Liu JP (1991) Bioequivalence and intrasubject variability. *J Biopharm Stat* **1:**205–219.
Matherly LH, Hou Z, and Deng Y (2007) Human reduced folate carrier: translation of basic biology to cancer etiology and therapy. *Cancer Metastasis Rev* **26:**111–128.
Matherly LH, Voss MK, Anderson LA, Fry DW, and Goldman ID (1985) Enhanced polyglutamylation of aminopterin relative to methotrexate in the Ehrlich ascites tumor cell in vitro. *Cancer Res* **45:**1073–1078.
Menter A, Korman, NJ, Elmets CA, Feldman SR, Gelfand JM, Gordon KB, Gottlieb AB, Koo JY, Lebwohl M, Lim HW, et al. (2009) Guidelines of care for the management of psoriasis and psoriatic arthritis: section 4, Guidelines of care for the management and treatment of psoriasis with traditional systemic agents. *J Am Acad Dermatol* **61:**451–485.
McGuire JJ, Hsieh P, Coward JK, and Bertino JR (1980) Enzymatic synthesis of folylpolyglutamates. Characterization of the reaction and its products. *J Biol Chem* **255:**5776–5788.
Mohsen MA (2010) A note on the calculation of intrasubject coefficient of variation in bioequivalence trials. *J Bioanal Biomed* **2:**75–78.
Nakai Y, Inoue K, Abe N, Hatakeyama M, Ohta KY, Otagiri M, Hayashi Y, and Yuasa H (2007) Functional characterization of human proton-coupled folate transporter/heme carrier protein 1 heterologously expressed in mammalian cells as a folate transporter. *J Pharmacol Exp Ther* **322:**469–476.
Narawa T and Itoh T (2010) Stereoselective transport of amethopterin enantiomers by the proton-coupled folate transporter. *Drug Metab Pharmacokinet* **25:**283–289.
Narawa T, Shimizu R, Takano S, Tsuda Y, Ono K, Yamada H, and Itoh T (2005) Stereoselectivity of the reduced folate carrier in Caco-2 cells. *Chirality* **17:**444–449.
Narawa T, Tsuda Y, and Itoh T (2007) Chiral recognition of amethopterin enantiomers by the reduced folate carrier in Caco-2 cells. *Drug Metab Pharmacokinet* **22:**33–40.
Olivry T, Paps JS, Bizikova P, Murphy KM, Jackson HA, and Zebala J (2007) A pilot open trial evaluating the efficacy of low-dose aminopterin in the canine homologue of human atopic dermatitis. *Br J Dermatol* **157:**1040–1042.
Piper JR and Montgomery JA (1974) A convenient synthesis of aminopterin and homologs via 6-(bromomethyl)-2,4-diaminopteridine hydrobromide. *J Heterocycl Chem* **11:**279–280.
Piper JR and Montgomery JA (1977) Preparation of 6-(bromomethyl)-2,4-pteridinediamine hydrobromide and its use in improved syntheses of methotrexate and related compounds. *J Org Chem* **42:**208–211.
Qiu A, Jansen M, Sakaris A, Min SH, Chattopadhyay S, Tsai E, Sandoval C, Zhao R, Akabas MH, and Goldman ID (2006) Identification of an intestinal folate transporter and the molecular basis for hereditary folate malabsorption. *Cell* **127:**917–928.
Qiu A, Min SH, Jansen M, Malhotra U, Tsai E, Cabelof DC, Matherly LH, Zhao R, Akabas MH, and Goldman ID (2007) Rodent intestinal folate transporters (SLC46A1): secondary structure, functional properties, and response to dietary folate restriction. *Am J Physiol Cell Physiol* **293:**C1669–C1678.
Rani S (2007) Bioequivalence: issues and perspectives. *Ind J Pharmacol* **39:**218–255.
Ratliff AF, Wilson J, Hum M, Marling-Cason M, Rose K, Winick N, and Kamen BA (1998) Phase I and pharmacokinetic trial of aminopterin in patients with refractory malignancies. *J Clin Oncol* **16:**1458–1464.
Rees RB, Bennett JH, Hamlin EM, and Maibach HI (1964) Aminopterin for psoriasis. A decade's observation. *Arch Dermatol* **90:**544–552.
Rieselbach RE, Morse EE, Rall DP, Frei E 3rd, and Freireich EJ (1963) Intrathecal aminopterin therapy of meningeal leukemia. *Arch Intern Med* **111:**620–630.
Smith A, Hum M, Winick NJ, and Kamen BA (1996) A case for the use of aminopterin in treatment of patients with leukemia based on metabolic studies of blasts in vitro. *Clin Cancer Res* **2:**69–73.
Swendseid ME, Swanson AL, Miller S, and Bethell FH (1952) The metabolic displacement of folic acid by aminopterin; studies in leukemia patients. *Blood* **7:**302–306.
Thiersch JB and Philips FS (1949) Effects of 4-amino-pteroylglutamic acid in dogs with special reference to megaloblastosis. *Proc Soc Exp Biol Med* **71:**484–490.
Von Hendy-Willson VE and Pressler BM (2011) An overview of glomerular filtration rate testing in dogs and cats. *Vet J* **188:**156–165.
Wang L, Cherian C, Desmoulin SK, Polin L, Deng Y, Wu J, Hou Z, White K, Kushner J, Matherly LH, et al. (2010) Synthesis and antitumor activity of a novel series of 6-substituted pyrrolo[2,3-*d*]pyrimidine thienoyl antifolate inhibitors of purine biosynthesis with selectivity for high affinity folate receptors and the proton-coupled folate transporter over the reduced folate carrier for cellular entry. *J Med Chem* **53:**1306–1318.
Zebala JA (2007) inventor; Syntrix Biosystems, assignee. Facile process for the preparation of high-purity aminopterin. United States patent 7,235**,**660. 2007 June 26.
Zhao R, Diop-Bove N, Visentin M, and Goldman ID (2011) Mechanisms of membrane transport of folates into cells and across epithelia. *Annu Rev Nutr* **31:**177–201.
Zhao R and Goldman ID (2007) The molecular identity and characterization of a Proton-coupled Folate Transporter–PCFT; biological ramifications and impact on the activity of pemetrexed. *Cancer Metastasis Rev* **26:**129–139.
Zhao R, Matherly LH, and Goldman ID (2009) Membrane transporters and folate homeostasis: intestinal absorption and transport into systemic compartments and tissues. *Expert Rev Mol Med* **11:**e4.

Address correspondence to: Dr. Stuart Kahn, Syntrix Biosystems, Inc., 215 Clay Street NW, Suite B-5, Auburn, WA 98001. E-mail: skahn@syntrixbio.com